The Effect of Forest on Mesoscale Rainfall: An Example from HAPEX–MOBILHY

E. M. BLYTH AND A. J. DOLMAN*

Institute of Hydrology, Wallingford, Oxon, United Kingdom

J. NOILHAN

Météo France, CNRM, Toulouse, France

(Manuscript received 31 December 1992, in final form 8 September 1993)

ABSTRACT

A meso-β-scale model is used to model a frontal intrusion in southwest France during HAPEX–MOBILHY. The skill of the model to reproduce the observed variation in temperature, humidity, and wind speed over the domain is reasonable within the limitations of the model parameterizations and initialization procedure, although there were errors in the timing and positioning of the front. A stable boundary layer was both observed and modeled over the forested area. The associated negative sensible heat flux provided the energy to sustain evaporation from the wet forest canopy under conditions of low radiation. A large wind shear over the stably stratified boundary layer provided the required turbulent kinetic energy to maintain the downward transport of sensible heat. Sensitivity experiments showed that local rainfall with a full forest cover changed from 2.9 to 3.8 mm, which represents a 30% increase when compared with a bare-soil domain. Half of this increase is from positive feedback of the intercepted water that reevaporates. The high roughness length of the forest, with its associated physical and dynamical effects, accounts for the rest of the increase in rainfall and for the accompanying increase in soil moisture.

1. Introduction

Experiments with atmospheric models have shown that forests can influence the climate. This influence may occur on a range of scales, from small local scales (de Bruin and Jacobs 1989), through mesoscales (André et al. 1989) to global scales (Rowntree 1988). On all these scales, physiognomic characteristics of the forests, such as surface conductance, aerodynamic roughness, and albedo, play an important role in determining the forest–atmosphere interaction. On a global scale, forests may also affect the hydrological balance of regions by increasing the rainfall (Sud et al. 1988).

Stewart (1977) was the first to demonstrate experimentally Rutter's (1967) suggestion that a forest, when its surface is wet, can draw energy from the overlying air to sustain its evaporation of intercepted rainfall. Such wet canopy evaporation is sustained by regional-scale advection of energy since the available energy in the form of net radiation is generally low under rainy conditions. The present study examines the possibility of modeling the behavior of a wet forest sufficiently accurately on the meso-β scale to reproduce the experimental evidence of regional-scale advection.

The increase of rainfall in the presence of forests at the mesoscale has not been studied extensively. André et al. (1989) modeled an increase in rainfall downwind of the Landes forest in southwest France. Two characteristics of the forest can cause an increase in rainfall. The high evaporation rate of intercepted water during rainfall can give a positive feedback, increasing the subsequent rainfall, and the high roughness length can result in enhanced water vapor convergence in the boundary layer, which can also increase the rainfall. The present paper attempts to show how important a role these two effects have in the rainfall at the meso-β scale.

The HAPEX–MOBILHY experiment in southwest France provides a convenient framework for investigating large-scale interactions of forests with the atmosphere and, in particular, for using a meso-β-scale model to understand the physics of this interaction. Previous mesoscale modeling of HAPEX–MOBILHY data has centered on the analysis of a "golden day," 16 June 1986, for which the conditions were markedly different from the present study day, with clear skies and high radiation levels. The ability of the model to simulate the main exchange processes of water and energy for several land use types under these dry condi-

* Current affiliation: The Winand Staring Centre for Integrated Land, Soil and Water Research, Wageningen, the Netherlands.

Corresponding author address: Dr. Eleanor M. Blyth, Institute of Hydrology, Crowmarsh Gifford, Wallingford, Oxfordshire, UK, OX10 8BB.

tions is excellent and has been documented in Bougeault et al. (1991a), Bougeault et al. (1991b), and Noilhan et al. (1991). In this paper the research version of the French Weather Service's mesoscale model, PERIDOT (Juvanon du Vachat et al. 1983), is used to simulate a frontal intrusion in the HAPEX–MOBILHY area on 5 June 1986.

2. Model description

The model has 30 levels in the vertical and with a grid size of 10 km covers an area of roughly 400 km × 400 km (Bougeault et al. 1991a). The time step is 60 s. Horizontal diffusion is applied using a Laplacian-type operator with a horizontal diffusion coefficient of 10^4 m^2 s^{-1}. The lateral boundary forcing is provided by a relaxation of the prognostic dynamic variables toward specified values on the boundaries of the domain (Davies 1976). These specified values change with time, and are provided by a larger-scale simulation model (Mercusot et al. 1986). The radiation code in the model distinguishes between clear sky and cloudy conditions and the calculation of vertical diffusion is based on the turbulent kinetic energy (TKE) scheme of Bougeault and Lacarrère (1989). The present study makes use of a large-scale precipitation scheme (Imbaud et al. 1987) where the precipitation flux is evaluated from a balance between condensation and evaporation of rainfall at each level. For the meso-β-scale experiments reported here, the deep convection parameterization is not used. The model was initialized with data from the 3D operational weather analysis of the French Weather Service, supplemented by the additional surface and radio sounding data obtained during the experiment (Mercusot et al. 1986). The particulars are shown in Table 1.

The land surface scheme is described in full by Noilhan and Planton (1989). Only those elements that relate to the interception of rainfall will be given here. The interception capacity of the vegetative canopy, $W_{r\max}$, is given by

$$W_{r\max} = 0.2(\mathrm{LAI})f_v, \tag{1}$$

where LAI is the leaf area index and f_v is the fraction of the grid covered by vegetation. A canopy interception reservoir W_r is filled by precipitation P and depleted by evaporation E_r:

$$\frac{\delta W_r}{\delta t} = Pf_v - E_r, \tag{2}$$

where δt is the time step. If the input to the reservoir is greater than the capacity, the extra rainfall is added to the throughfall. Following Deardorff (1978) the interception reservoir covers only a fraction $f_v\Delta$ of the grid square:

$$\Delta = \left(\frac{W_r}{W_{r\max}}\right)^{2/3}. \tag{3}$$

Evaporation E_r of intercepted rainfall from the reservoir is parameterized as:

$$E_r = \frac{f_v\Delta[q_{\mathrm{sat}}(T_s) - q_a]}{r_a},$$

where $q_{\mathrm{sat}}(T_s)$ is the saturated humidity at the surface temperature T_s, q_a is the specific humidity at the lowest model layer, and r_a the aerodynamic resistance to water vapor transport. Mahfouf and Jacquemin (1989) describe a detailed validation of the interception parameterization over agricultural crops in the HAPEX square.

For the modeling program of HAPEX–MOBILHY, a particular effort was paid to obtain maps of vegetation and soil properties in the area of interest. A detailed description of the methods used to obtain the necessary surface information from two classifications for the vegetation and for the soil texture can be found in Bougeault et al. (1991a).

The initial values of the soil water content for the two soil layers of the model (a thin surface layer and a deep reservoir) were taken from observations of the soil moisture, available every week at 12 sites within

TABLE 1. Particulars of the PERIDOT meso-β-scale model.

Number	Item	Description	Reference
1	Horizontal resolution	10 km at 60° to 9 km at 45°	
2	Vertical resolution	30 σ levels $\Delta z \approx$ 100 m below 2000 m	
3	Domain	43 × 43 grid points	
4	Time step	60 s	
5	Radiation		Geleyn and Hollingsworth (1979)
6	Clouds		Slingo (1980)
7	Precipitation		Imbaud et al. (1987)
8	Turbulence		Bougeault and Lacarrère (1989)
9	Soil classification	Clapp and Horberger	Bougeault et al. (1991a)
10	Land surface scheme	NP89	Noilhan and Planton (1989)
11	Surface stability		Louis et al. (1981)
12	Lateral boundary conditions		Davies (1976)

the experimental area. At the beginning of June, the observed moisture content was close to the field capacity, both for the loamy and sandy soils of the area under study. The initial values of the two soil reservoirs were set to 0.75 of the saturated water content of the soil type within each grid box. This rather crude method is necessary since a specific assimilation of soil moisture is not yet available. However, the possible errors in the initial water content are not of great significance in this study since the results of the simulation rely on the short-term response of intercepted water and high evaporation rate over bare ground.

3. Comparison of model predictions with observations

a. Synoptic situation on 5 June 1986

The synoptic situation over the HAPEX square in France for 5 June 1986, the day chosen for simulation, is described by Cazalens and Sejourné (1987). At 500 hPa (Fig. 1a) a depression extended from the North Sea to north Italy and a high, centered on the Azores in the Atlantic, reached up to Iceland giving a north-northwest wind of 65 kt through France. The situation at ground level was similar, as shown in Fig. 1b. These pressure fields had been established on the previous day, when a front passed over the HAPEX square producing a small amount of rainfall (2 mm). On 5 June it rained more heavily (6 mm). The pressure fields indicate a weak, cold front moving southeastward over France, arriving at the HAPEX square at about 0900 UTC. At 1200 UTC it lay across the middle of the HAPEX square and subsequently moved south and east to the Mediterranean.

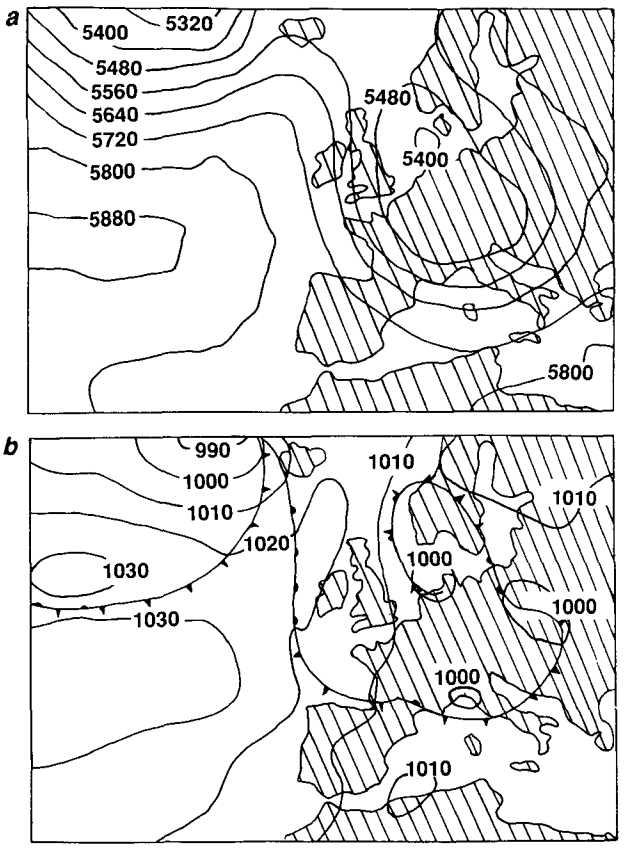

FIG. 1. (a) Contours of height (m) at 500 hPa and (b) contours of pressure (hPa) at surface at 1200 UTC 5 June 1986.

b. Comparison with surface data

Goutorbe and Tarrieu (1991) give a summary of the data available for assessing model performance. Measurements of humidity, temperature, short- and longwave radiation, and wind speed are available for most of the surface stations in the HAPEX square. Although latent and sensible heat fluxes were measured at some locations, they have low reliability under the conditions prevailing on 5 June and consequently no comparison with flux data is given.

Figure 2 shows the fields of wind velocity and temperature from the observations and the model at 1200 UTC. The coastline and the HAPEX square are shown in this and subsequent figures to aid orientation. The front lies east–west roughly halfway between the top and bottom of the figures. Conditions before the front are moist, warm (14°C), and cloudy with a strong wind (above 10 m s^{-1}) from the west. Behind the front the air is cooler (12.5°C) and drier, the sky is clear, and the wind is weak (less than 5 m s^{-1}) and from the north. At 1200 UTC, the model shows a similar trend with predicted temperatures before the modeled front of about 13.5°C and a westerly wind of over 10 m s^{-1}. Behind the modeled front the temperatures are about 12°C and the northerly wind is less than 5 m s^{-1}. The modeled transition between these conditions is farther to the north, however, and does not extend as far to the west as was observed.

Figures 3a and 3b show observed and modeled cumulative rainfall over the day. The observed daily total was about 6 mm, with high values in the south in the region of high mountain range of the Pyrennées. The modeled daily total is about 6 mm in the northern part of the domain and exceeds 20 mm over the Pyrennées mountains. Rainfall is difficult to model, and the fact that the modeled daily rainfall is close to that observed is reassuring. The distribution of rainfall is also in qualitative agreement with the observed rainfall pattern. It is interesting to note the prediction of higher total rainfall near the west coast. However, the position of the modeled frontal rainfall (i.e., the rainfall not associated with the coast, the Pyrennées, and the Massif Central) is too far east, an error that relates to the general mispositioning of the front in the model.

Locally, a comparison can be made of the observed and modeled time series of temperature, humidity, and wind speed. This is shown in Fig. 4 for the central site,

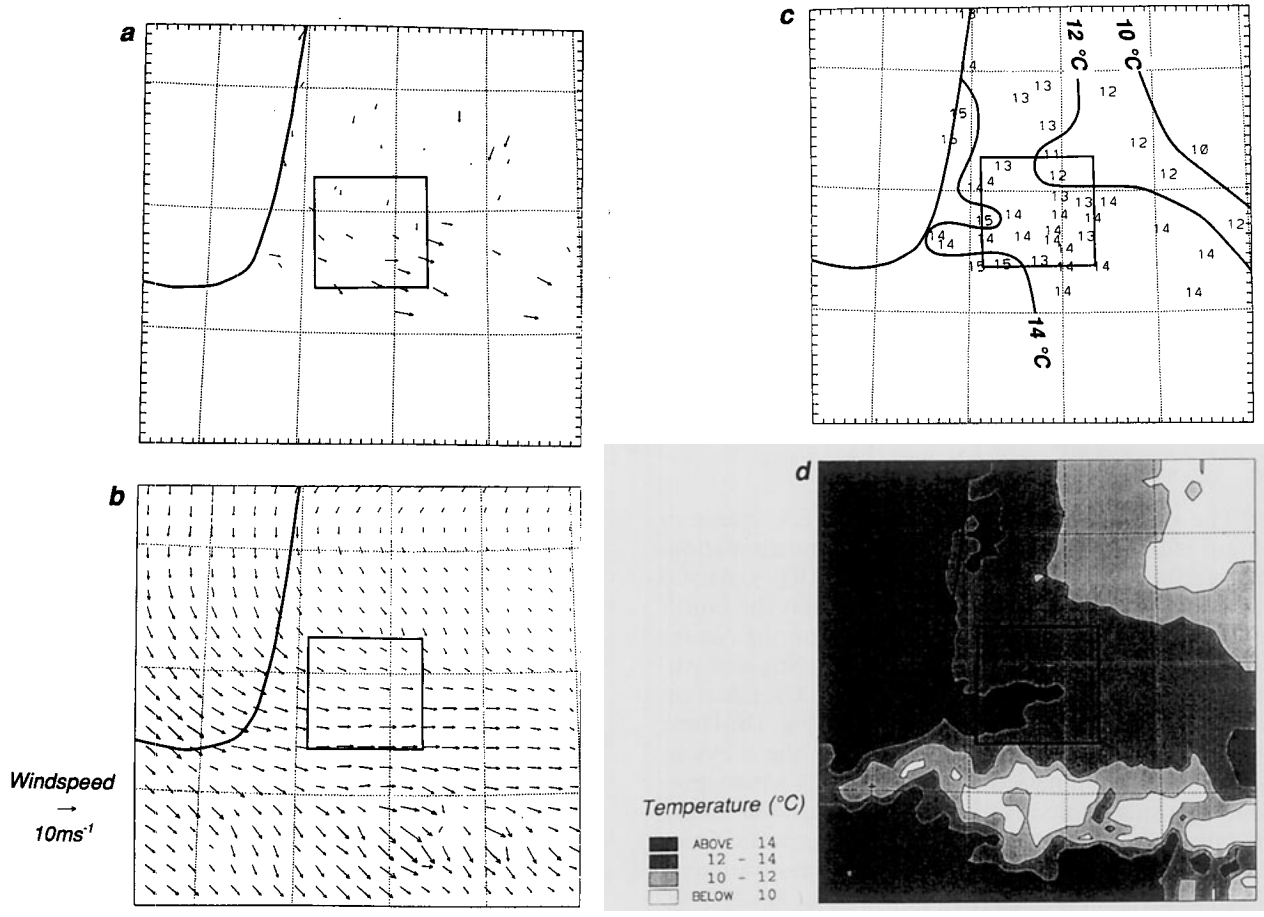

FIG. 2. Fields of wind vectors (m s^{-1}) at 1200 UTC (a) observed and (b) modeled and of temperatures (°C) at 1200 UTC (c) observed and (d) modeled.

which is in the top right-hand quarter of the HAPEX square. There is evidence of the frontal passage in the observations; the wind speed, humidity, and temperature are all relatively high between 1000 UTC and midday and when the front passes at 1200 UTC, all three variables decrease. The signal is strongest in the wind speed time series and weakest in the temperature time series.

The time series of wind speed, humidity, and temperature obtained by the model, which is near the central site, show the frontal passage less clearly. The magnitude of the variables are roughly consistent with the observations; the modeled humidity agrees very well with the observations while wind speed and temperature in particular show much less variation than the observations. The local minima in the temperature, humidity, and wind speed series, which represents the arrival of the front, can be observed at 1400 UTC, which is 2 h later than in the observations. Noilhan et al. (1991) have already noted the problems involved in comparing local surface data with observations in the clear-sky case of 16 June. The present study, which is much more dependent on the dynamical and spatial features of the frontal passage, makes such a comparison even more hazardous.

The modeled water content W_r of the interception reservoir is shown in Figs. 5a and 5b. At 1000 UTC, when light rain is falling throughout the domain, the interception reservoir is a function of the surface cover; high over the forested areas (the forest is identified with areas of high roughness length in Fig. 10) and low over the sparsely vegetated agricultural areas. At 1400 UTC the cloud and resulting radiation and rainfall patterns in the model are more complex. There are clear sky conditions over the north of the domain and the intercepted water on the canopies in these areas has now evaporated. Bands of cloud and rain associated with the front appear across the Landes forest (Fig. 5b) resulting in well-defined bands of W_r. Bands of cloud resembling the modeled cloud in position, orientation, and dimension were observed in Meteosat images.

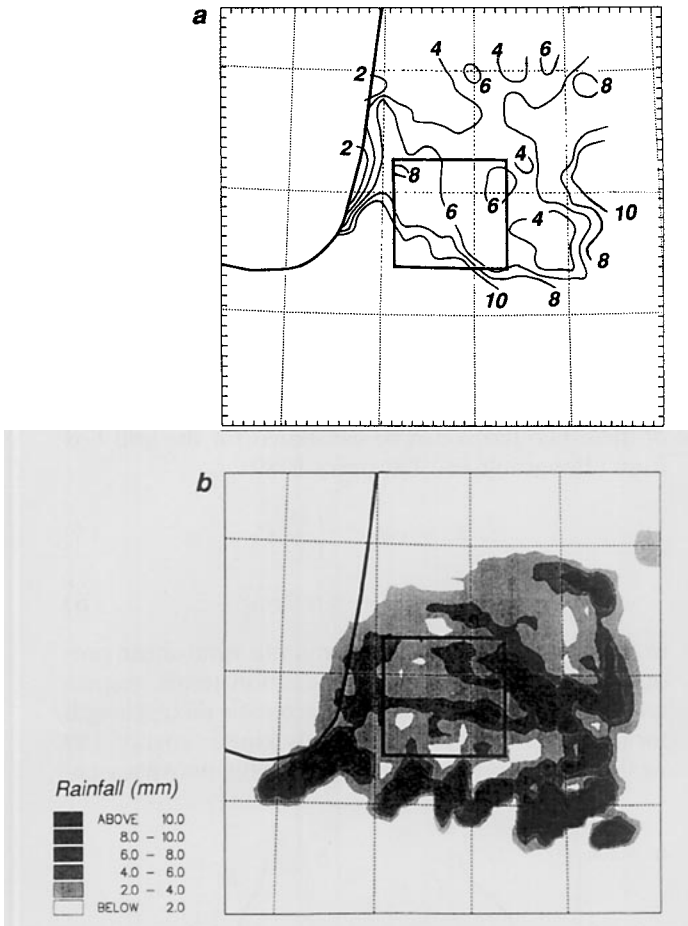

FIG. 3. Fields of cumulative rainfall (mm) (a) observed and (b) modeled.

c. *Boundary-layer structure*

At the HAPEX–MOBILHY central site eight radiosoundings per day were made to determine the diurnal cycle of the boundary-layer structure. Previous analysis (Brutsaert et al. 1988) has suggested that, at least for clear sky conditions, the boundary-layer structure as measured by the radiosondes was strongly determined by the forest that surrounded the launch site in a forest clearing.

Figure 6 shows the time evolution of the measured profiles of potential temperature, humidity, and wind speed and direction at the central site for 5 June. Figure 6a shows that the boundary layer is strongly stable at the early morning observation and is slightly less stable during the rest of the day. The arrival of maritime air between 0500 and 1100 UTC involves a progressive heating and moistening of the lower layers (Figs. 6a and 6b). Note the slight destabilization of the first 500 m (975 mb) of the boundary layer. The 1700 UTC sounding is taken after the passage of the front and shows a cooler and drier boundary layer. The wind speed is less at 1700 UTC and it has rotated to the north (Figs. 6c,d).

Figure 7 shows the modeled profiles for a fully forested grid near the central site. It has already been shown that there is a time lag of about 2 h between the modeled and observed movement of the front. This is reflected in the structure of the modeled boundary layer. The modeled wind speeds at the upper layers at 0500 and 1100 UTC are low by almost a factor of ⅔ (Fig. 7c). This is probably due to relatively poor initialization of the model by its lateral boundary conditions (Mahfouf 1988). In consequence the modeled lateral advection of cooler air does not take place at

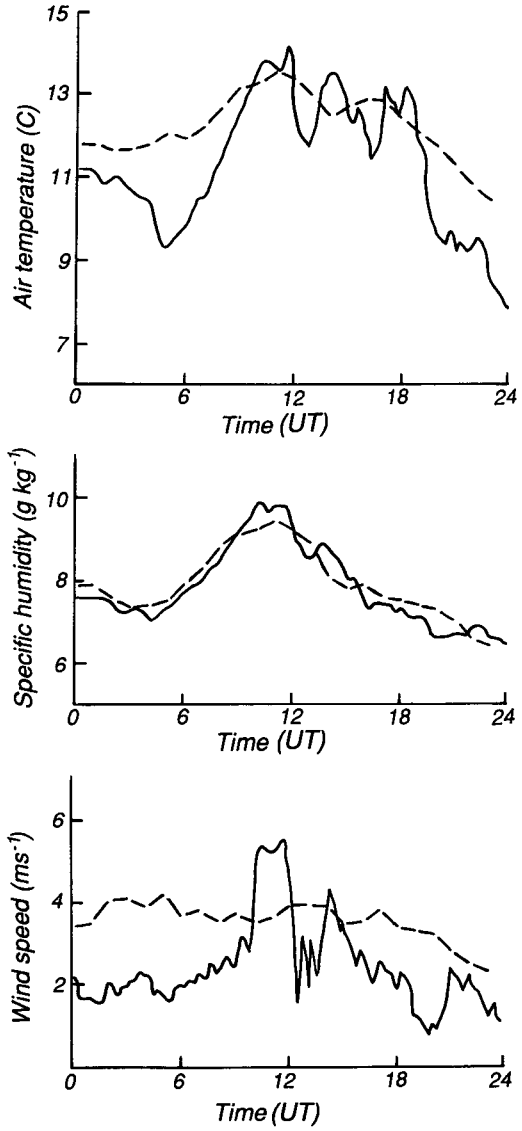

FIG. 4. Time evolution of (a) wind speed at 10 m, (b) temperature at 2 m, and (c) specific humidity at 2 m. The dashed lines are the model predictions at position (25, 26); the solid lines are the observations at the central site.

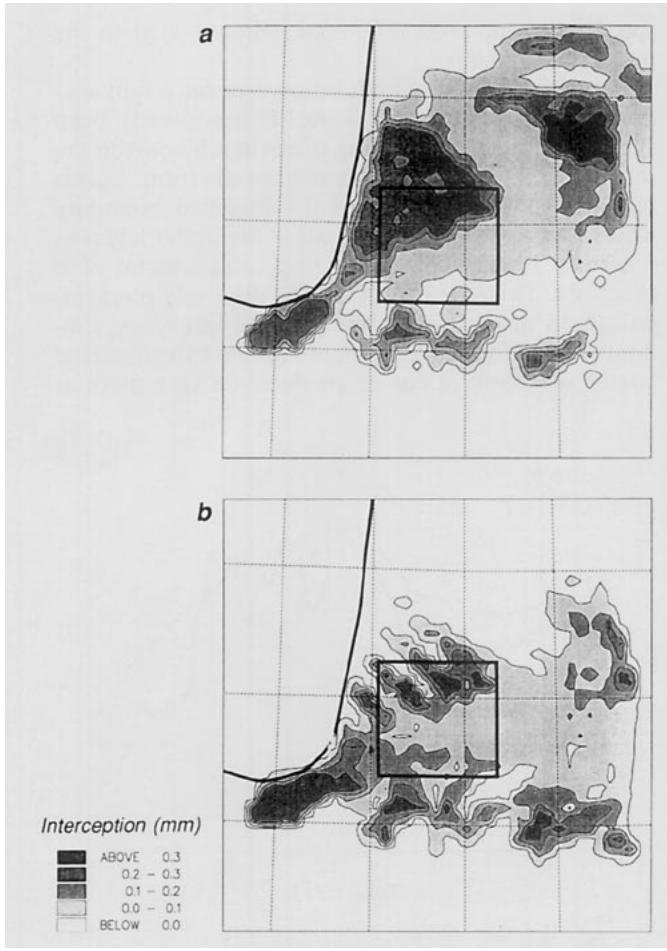

FIG. 5. Contours of modeled interception capacity (mm) at (a) 1000 UTC and (b) 1400 UTC.

the observed rate. The model does, however, reproduce the stable structure of the boundary layer and the heating and moistening between 0500 and 1100 UTC followed by a cooling and drying (Figs. 7a,b). The model does not reproduce the rotation of the wind to the north in the afternoon, but rather predicts a north-northwest flow, consistent with its error in positioning the front (Fig. 7d).

4. Interception: Surface–atmosphere interaction over the forest

The observed and modeled stable boundary-layer structure (Figs. 6a and 7a) over the forest is a result of the combination of synoptic weather conditions and the interaction of the forest with the lowest layers of the atmosphere. The wet forest evaporates at a high rate, cooling the surface relative to the warmer overlying air. The radiation received at the surface and heat storage in the forest are not sufficient to maintain these high evaporation rates and energy is drawn from the warmer air passing over the forest. This is shown in Fig. 8 where the sensible and latent heat flux profiles are shown for a fully forested grid adjacent to the central site. A positive latent heat flux at the surface of about 80 W m^{-2} is coupled with a negative sensible heat flux bringing heat downward to the evaporating surface. These evaporation rates are of similar magnitude as those observed by Stewart (1977) for a wet canopy at Thetford Forest.

The supply of warm air to the evaporating surface can only be maintained if there is downward entrainment of warm air into the stable layer by turbulence. The turbulent kinetic energy (TKE) budget is dominated by two terms, the buoyancy term and the dynamical wind-shear production term. The magnitude of these two terms can be calculated for the grid box from (Bougeault and Lacarrère 1989):

$$P_d = c_k l_k e^{1/2} \left(\frac{\delta u}{\delta z} \right)^2 \tag{5}$$

$$P_b = \beta(\overline{w'\theta'} + 0.608\overline{w'q'}), \tag{6}$$

in which P_d and P_b are the dynamic wind-shear production and the buoyancy production terms, respectively, c_k is a constant, l_k is a characteristic mixing length for the eddies, e is the mean eddy kinetic energy, $\delta u/\delta z$ the wind speed gradient, and β is the buoyancy pa-

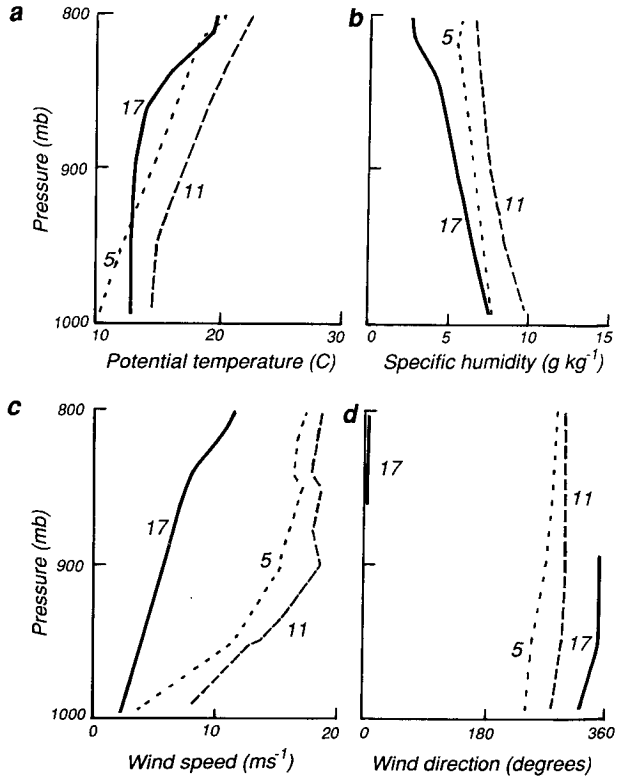

FIG. 6. Observed profiles at central site at 0500, 1100, and 1700 UTC of (a) temperature, (b) humidity, (c) wind speed, and (d) wind direction.

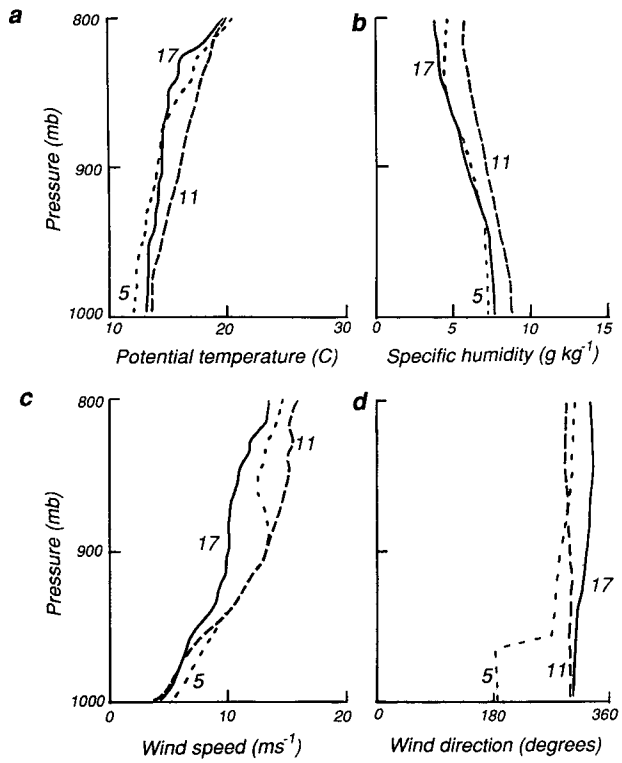

FIG. 7. Modeled profiles at position (24, 25) at 0500, 1100, and 1700 UTC of (a) temperature, (b) humidity, (c) wind speed, and (d) wind direction.

rameter, while $w'\theta'$ and $w'q'$ are the eddy fluxes of heat and water vapor and k is the von Kármán constant.

Using modeled values for the variables used in (5) and (6), the buoyancy term P_b is -0.5×10^{-3} m^2 s^{-3} and the wind-shear term P_d is 1.2×10^{-3} m^2 s^{-3}. The stable layer is therefore a sink for turbulence. The large gradient in wind speed over the forest (Fig. 7c) provides the mechanism for the entrainment of warm air. The resulting TKE profile is greater than zero in the lower boundary layer (Fig. 8c), which sustains the downward transport of sensible heat to the wet forest canopy. It is interesting to note that this downward transport of sensible heat could only have been modeled with a TKE parameterization of the diffusion coefficients, since a parameterization based on stability would probably reduce the vertical diffusion too much, and result in a much more stable boundary layer.

The present model results provide evidence for the maintenance of wet canopy evaporation from forests through a negative sensible heat flux and show, perhaps more importantly, how local-scale processes can be linked to mesoscale meteorological phenomena.

5. Sensitivity of mesoscale rainfall to land surface cover

André et al. (1989) have shown that there may be an increase in rainfall downwind of a forest. They suggested that the primary mechanism for this influence was an increase in humidity of the air downwind of the forest, as a result of rapid evaporation of intercepted rainfall. However, an increase in roughness length may also increase the precipitation by a change in the boundary-layer water vapor convergence. Note, however, that the increased evaporation is in part also a roughness effect as it is predominantly the high aerodynamic conductance of forest that gives rise to high evaporation rates from wet canopies.

To quantify the relative importance of these two effects, three sensitivity tests were carried out. In these tests the land surface in the model domain was replaced by a homogeneous surface cover. Forest and bare ground were used to represent surfaces with maximum and minimum potential for feedback, respectively. Also a hypothetical surface was used that had the same roughness as the forest but no interception capacity, causing the evaporation rates to be lower than from the bare-soil run. This was intended to isolate the two feedback mechanisms of high roughness and high evaporation rates. The same large-scale forcing was used in each case. The values of the surface parameters, W_r and z_0, for the three sensitivity runs and mean values for the control run are given in Table 2.

The spatial distribution of the rainfall for three of the runs (control, forest, and bare ground) is shown in Fig. 9. There is an area of rainfall on the coastline

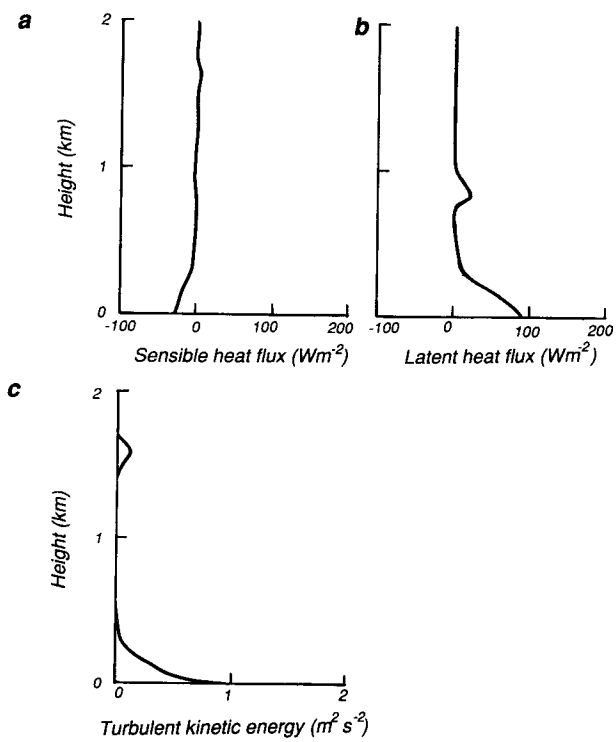

FIG. 8. Modeled profiles at position (24, 25) at 1500 UTC of (a) sensible heat flux, (b) latent heat flux, and (c) turbulent kinetic energy.

TABLE 2. Sensitivity experiments. Rainfall (mm) is computed for subdomain. Parameter values are averaged over full domain.

Experiment	z_0 (m)	$W_{r\max}$	P (mm)	Δm	E_{tot}
Control	0.276	0.17	3.3	1.42	1.89
Forest	1.0	0.46	3.8	1.93	1.83
Bare soil	0.01	0.0	2.9	1.22	1.68
Forest (W_r = 0)	1.0	0.0	3.4	1.94	1.46

in both the control run and the forest run. This is likely to be solely a result of the increased roughness length of the forested area in that part of the domain as the area over which this precipitation develops is not large enough to create a substantial humidity feedback. This rainfall is not associated with the front that is positioned farther to the east. In the eastern frontal region the forested run simulates more rainfall than either the bare soil or control run. Unlike the rainfall on the coastline, this is likely to be caused by a combination of both the humidity feedback and the roughness length.

To quantify these two effects a comparison is made of the water balance between the three sensitivity runs.

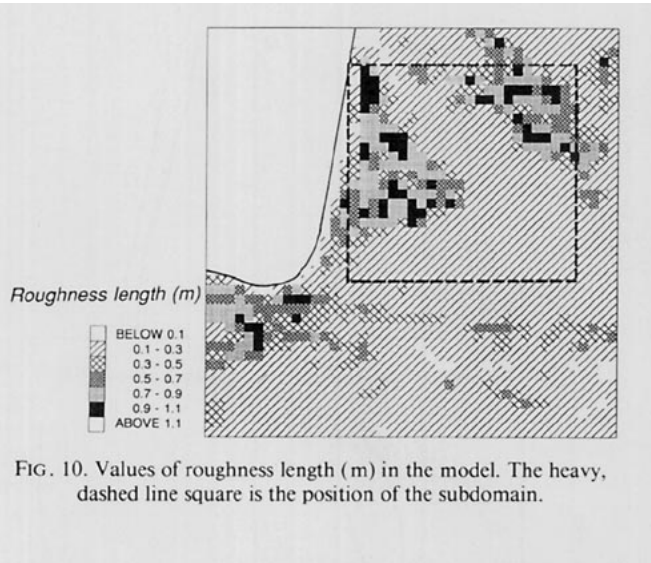

FIG. 10. Values of roughness length (m) in the model. The heavy, dashed line square is the position of the subdomain.

To assess sensitivity that avoids the effects of the sea and the mountain ranges of the Pyrenees and the Massif Central, a subdomain of the model was chosen (Fig. 10). These exclusions allow the influence of the land surface cover to be separated form the orographic effect.

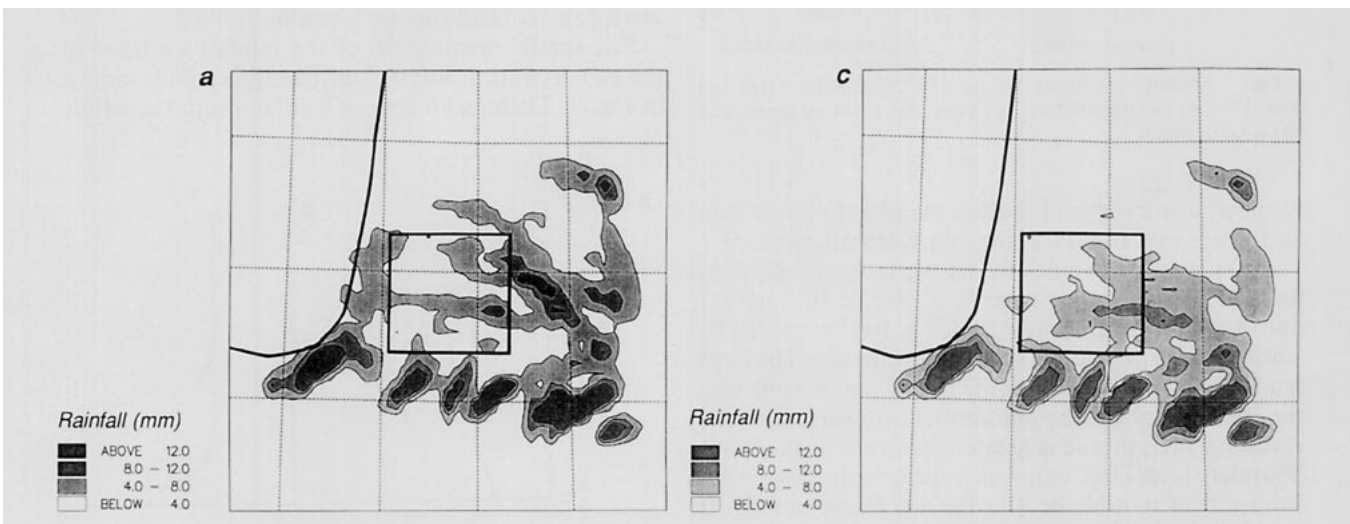

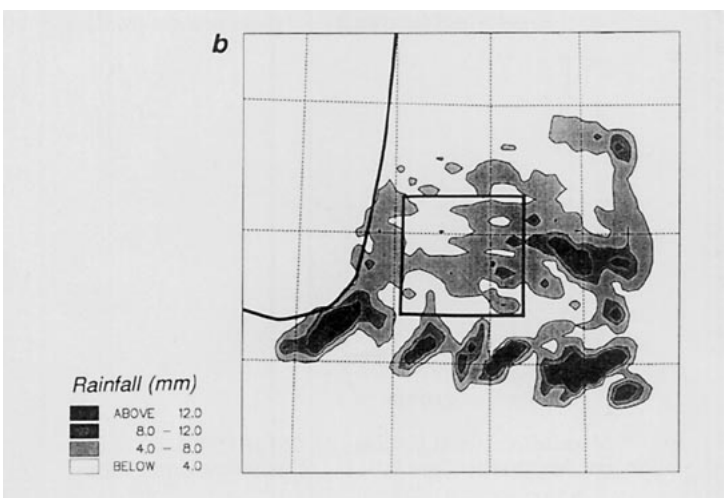

FIG. 9. Contours of cumulative modeled rainfall (mm) for (a) the control run, (b) the forest run, and (c) the bare-soil run.

The daily rainfall, the change in soil moisture, and the daily evaporation of the three sensitivity runs are shown in Table 2.

The forest run produces more rainfall (3.8 mm) than the forest without interception (3.4 mm), although the increase in soil moisture is the same (1.94 mm). This implies that the extra rainfall caused by the feedback of the evaporation of intercepted water is merely recycled within the boundary layer and does not enter the soil. The forest without interception produces more rainfall than the bare soil (2.9 mm), although the evaporation is equal or less throughout the day. This implies that the high roughness length of the forest plays a significant role in increasing the rainfall. The increase in soil moisture of the bare-soil run is 0.7 mm less than that of the forest without interception. Of that total 0.5 mm is due to the difference in rainfall and 0.2 mm is due to the high evaporation rates of the bare soil after the rainfall event.

From these runs it can be tentatively concluded that of the 30% increase in rainfall between the forest run and the bare-soil run about half is recycled through interception and evaporation back to the atmosphere and does not reach the soil. The other half, caused by the increase in roughness length, represents a net gain of water to the land from the atmosphere.

6. Discussion

The comparison of the modeled variables with observations showed that it is possible to model the salient features of a frontal intrusion in the HAPEX–MOBILHY area. The total daily rainfall and variation of cloud cover and radiation were modeled with reasonable accuracy. The exact timing and position of the front were in some error, however. This is likely to be caused by the initialization of the model. A comparison with modeled and observed wind speeds (Fig. 2) shows that the modeled winds have too strong a westerly component, pushing the front too far to the east. At the same time, an underestimation of the northerly component causes the arrival of the front to be delayed by about 2 h.

The present study provides evidence of the mechanism for maintaining negative sensible heat flux over forest, which is capable of sustaining wet canopy evaporation when the radiation is low. The main condition needed for this mechanism to occur is a strong wind shear within a stably stratified boundary layer. Such conditions are likely to occur when relatively strong winds in the boundary layer are associated with a wet surface with a high aerodynamic roughness, such as a forest. How great the wind shear needs to be to initiate or sustain will depend on the magnitude (negative) of the buoyancy term in the TKE budget equation as the (positive) dynamical contribution should exceed this. This provides the mechanism for downward transport of heat and upward evaporation. PERIDOT was able to model this effect because the vertical diffusion parameterization is dependent on the turbulent kinetic energy.

This mechanism will probably occur when the size of a forest exceeds a certain critical limit. For instance, the control run shows that the size of Les Landes forest is sufficient to create this mechanism. Typically, the boundary layer responds to surface length scales in the order of 10–20 km. As this also corresponds to the size of a model grid box in this experiment, this provides a lower limit of 10–20 km for the size of a forest. How much smaller this length scale can be is not clear and can only be resolved by measurements over small areas of forest or model experiments with a higher resolution.

The results of the sensitivity experiments show that forests can have a considerable effect on the rainfall in a frontal situation. The total rainfall, when the surface was covered by forest, was 30% higher than when the surface was all bare soil. It was demonstrated that the higher evaporation rates from a wet forest during a rainfall event accounts for about half of that increase but does not contribute to an increase in soil moisture. It is postulated here that convergence of water vapor in the boundary layer due to the high roughness of the forest accounts for the other 50% of the increase in rainfall, which increases the soil moisture.

It should be stressed that these results were obtained for a specific case, with a specific set of initial conditions and model parameterizations. Further work should be done to test the generality of these conclusions. It is tempting, however, to speculate on the possible consequences of the present results. The increased rainfall recycling from a positive humidity feedback will have effects on the regional rainfall dynamics and patterns, and is thus of considerable importance in regional (high resolution) weather prediction models. The effect of the roughness lengths can influence the long-term water balance, however, as it provides a net gain of water by the land from the atmosphere. This latter effect is of considerable importance in predicting the effect of land use changes on climate (e.g., Rowntree 1988). As before, the size of the forest patch required to obtain this effect is not well known. As it is likely that extra water vapor convergence within the boundary layer is the main cause for this effect, it is likely that the same arguments as used before apply and that the minimum size of the forest should be of the order of 10–20 km. Exactly how the amount of rainfall is related to the size of the forest remains unknown and currently highly speculative.

Acknowledgments. The authors are pleased to acknowledge the support of the British–French Alliance Programme. AJD and EMB are supported by a CEGB Senior Research Fellowship, funded by the Joint Environmental Programme of National Power and PowerGen (United Kingdom).

REFERENCES

André, J.-C., P. Bougeault, J.-F. Mahfouf, P. Mascart, J. Noilhan, and J.-P. Pinty, 1989: Impacts of forests on mesoscale meteorology. *Philos. Trans. Roy. Soc. London,* **B 324,** 407–422.

Bougeault, P., and P. Lacarrère, 1989: Parameterisation of orography-induced turbulence in a meso-β-scale model. *Mon. Wea. Rev.,* **117,** 1872–1890.

——, J. Noilhan, P. Lacarèrre, and P. Mascart, 1991a: An experiment with an advanced surface parameterization in a mesobeta-scale model. Part I: Implementation. *Mon. Wea. Rev.,* **119,** 2358–2373.

——, B. Bret, P. Lacarèrre, and J. Noilhan, 1991b: An experiment with an advanced surface parameterization in a mesobeta-scale model. Part II: The 16 June 1986 simulation. *Mon. Wea. Rev.,* **119,** 2374–2392.

Brutsaert, W., M. B. Parlange, and J. H. C. Gash, 1988: Neutral humidity profiles in the boundary layer and regional evaporation of sparse pine forest. *Ann. Geophys.,* **7,** 623–630.

Cazalens, R., and B. Sejourné. 1987: Programme HAPEX–MOBILHY. Atlas des situations synoptiques, 73 pp. [available from CNRM, 42, av. Coriolis, 31057 Toulouse, France.]

Davies, H. C., 1976: A lateral boundary formulation for multi-level prediction models. *Quart. J. Roy. Meteor. Soc.,* **102,** 405–418.

de Bruin, H. A. R., and C. M. J. Jacobs, 1989: Forest and regional scale processes. *Philos. Trans. Roy. Soc. London,* **B324,** 393–406.

Deardorff, J. W., 1978: Parameterization of the planetary boundary layer for use in general circulation models. *Mon. Wea. Rev.,* **100,** 93–104.

Geleyn, J. F., and A. Hollingsworth, 1979: An economical analytical method for the computation of the interaction between scattering and line absorbtion radiation. *Contrib. Atmos. Phys.,* **52,** 116–131.

Goutorbe, J-P., and C. Tarrieu, 1991: HAPEX–MOBILHY data base. *Land surface evaporation: Measurement and parameterization,* J.-C. André and T. Schmugge, Eds., Springer Verlag, 403–410.

Imbaud, M., A. Craplet, P. Degardin, Y. Durand, A. Joly, N. Marie, and J. F. Geleyn, 1987: Fine-mesh limited area forcasting with the French operational PERIDOT system. The nature and prediction of extra-tropical weather systems. [Available from ECMWF, Shinfield park, Reading, UK.]

Juvanon du Vachat, R., A. Craplet, Y. Durand, A. Joly, L. Pham, and D. Rouseau, 1983: Fine mesh numerical weather prediction over France. *Sixth Conf. Numerical Weather Prediction.* Amer. Meteor. Soc., Omaha, NE, 57–61.

Louis, J. F., M. Tiedtke, and J. F. Geleyn, 1981: A short history of the operational PBL parameterization at ECMWF. *Workshop on Planetary Boundary layer Parameterization,* Reading, UK, *ECMWF,* 59–79.

Mahfouf, J. F., 1988: Etude des situations pertubées d'HAPEX–MOBILHY, 165 pp. [Available from CNRM, 42, av. Coriolis, 31057 Toulouse, France.]

——, and B. Jacquemin, 1989: A study of rainfall interception using a land surface parameterization for mesoscale meteorological models. *J. Appl. Meteor.,* **28,** 1282–1302.

Mercusot, C., P. Bougeault, and Y. Durand, 1986: Programme HAPEX–MOBILHY, atlas des donées PERIDOT, 269 pp. [Available from CNRM, 42, av. Coriolis, 31057 Toulouse, France.]

Noilhan, J., and S. Planton, 1989: A simple parameterization of land surface processes for meteorological models. *Mon. Wea. Rev.,* **117,** 536–549.

——, P. Lacarrere, and P. Bougeault, 1991: An experiment with an advanced surface parameterization in a mesobeta-scale model. Part III: Comparison with the HAPEX–MOBILHY dataset. *Mon. Wea. Rev.,* **119,** 2393–2413.

Rowntree, P. R., 1988: Review of general circulation models as a basis for predicting the effects of vegetation change on climate. *Forests, Climate and Hydrology: Regional impacts,* E. R. C. Reynolds and F. B. Thompson, Eds., Kefford Press, 162–193.

Rutter, A. J., 1967: An analysis of evaporation from a stand of Scots pine. *International Symposium of Forest Hydrology.* W. E. Sopper and H. W. Lull, Eds., Pergamon Press, 403–417.

Slingo, J. M., 1980: A cloud parameterization scheme derived from GATE data for use with a numerical model. *J. Appl. Meteor.,* **18,** 639–646.

Stewart, J. B., 1977: Evaporation from the wet canopy of a pine forest. *Water Resour. Res.,* **13,** 915–921.

Sud, Y. C., J. Shukla, and Y. Mintz, 1988: Influence of land surface roughness on atmospheric circulation and precipitation: A sensitivity study with a general circulation model. *J. Appl. Meteor.,* **27,** 1036–1054.